Journal of Photochemistry and Photobiology A: Chemistry 206 (2009) 53–63

Contents lists available at ScienceDirect

Journal of Photochemistry and Photobiology A: Chemistry

journal homepage: www.elsevier.com/locate/jphotochem

Effect of counter electrode, thickness and sintering temperature of TiO_2 electrode and TBP addition in electrolyte on photovoltaic performance of dye sensitized solar cell using pyronine G (PYR) dye

P. Balraju [a], P. Suresh [a], Manish Kumar [b], M.S. Roy [b], G.D. Sharma [a,*,1]

[a] Molecular Electronics and Optoelectronics Device Laboratory, Department of Physics, JNV University, Jodhpur, Rajasthan 342005, India
[b] Defence Laboratory, Jodhpur, Rajasthan, India

ARTICLE INFO

Article history:
Received 22 August 2008
Received in revised form 25 April 2009
Accepted 12 May 2009
Available online 22 May 2009

Keywords:
Dye sensitized solar cells
Effect of counter electrode
Photovoltaic effect
Additives

ABSTRACT

Dye sensitized solar cells (DSSCs) assembled with nano-crystalline TiO_2 adsorbed with pyronine G (PYR) dye as photoanode and polar solvent-treated poly(3,4-ethylene dioxythiophene):poly(styrene sulfonate) (PEDOT:PSS) coating on a conductive glass (fluorine-doped thin oxide, FTO), as a counter electrode were studied. It was found that the DSSC using carbon black (0.2 wt%) modified DMSO-PEDOT:PSS conductive coating as a counter electrode resulted highest power conversion efficiency. This is attributed to the role of DMSO in enhancing the conductivity of a PEDOT:PSS film and carbon black plays a vital role in increasing the catalytic activity of the film due to its larger surface area. The solar cell performance was studied as a function of sintering temperature and thickness of TiO_2 layer, dye sensitization time of TiO_2 electrode and electrolyte composition. The DSSCs consist of TiO_2 electrode sintered at a temperature of 450 °C shows higher photocurrent attributed to the formation of higher crystalline film. This enhancement in the interconnection between particles results a swift diffusion of electrolyte and good transportation of electrons in the film. All types of DSSC possess the same dependence of performance on the photoanode thickness, i.e. the efficiency increases with the anode thickness to a maximum value, and then decreases slightly when the thickness of photoanode increases further. The effect of pyridine derivative addition in electrolyte on the performance of photovoltaic parameters of DSSCs has also been investigated. A reduced interface defect density and a resulting reduction of charge carrier recombination were found to be the main mechanism for an increased open circuit voltage of DSSCs with TBP addition in the electrolyte. The negative shift of conduction band edge of TiO_2 after the addition of TBP in electrolyte was also to be a factor in improving the open circuit voltage. The over all power conversion efficiency of the DSSCs with TBP in the electrolyte is about 5.24%.

1. Introduction

The dye sensitized solar cell (DSSC) is a device for the conversion of visible light into electricity based on the sensitization of wide band gap semiconductors [1]. The structure of DSSC is consistent with a counter electrode of conductive glass coated with platinum (Pt), a photoanode of TiO_2 porous film on a conductive glass substrate anchored a monolayer of dye and an electrolyte of certain organic solvent containing a redox couple such as iodide/triiodide. The absorption spectrum of the dye and anchoring of the dye to the surface of TiO_2 are important parameters determining the efficiency of the cell [2]. Nano-crystalline TiO_2, has been extensively investigated as a potential material for dye sensitized solar cells [3,4].

When a DSSC is irradiated by sunlight, the electrons of the dye are excited from ground state to excited state by absorbing the photons. The excited electrons are injected into the conduction band of TiO_2 porous film and then transferred to the conducting glass through the porous TiO_2 film. In a DSSC, a sputtered platinum (Pt) coated conducting glass is usually employed as a counter electrode of the DSSC to catalyse the reduction of I_3^-/I^- in redox electrolyte. However, Pt is one of the expensive rare metals in the earth; the use of the counter electrodes with other cheaper materials expected to reduce the production cost of the device is needed. Therefore, Yahannes and Inganes [5] have reported that the electrochemically polymerized and doped poly(3,4-ethylene dioxythiophene) (PEDOT) can catalyse the reaction of I_3^-/I^- redox couple in DSSCs. It is also reported that conducting polymers such as PEDOT, polypyrrole (PPy) and polyaniline (PANI) can be substituted for the sputtered platinum counter electrode of DSSC [6]. PEDOT

* Corresponding author. Present address: Director, Jaipur Engineering College, Kukas, Jaipur. Tel.: +91 0291 2720857.
E-mail address: sharmagd_in@yahoo.com (G.D. Sharma).
[1] On sabbatical leave from JNV University, Jodhpur.

1010-6030/$ – see front matter © 2009 Elsevier B.V. All rights reserved.
doi:10.1016/j.jphotochem.2009.05.014

doped poly(4-styrene sulfonate) (PEODT:PSS) has also attracted much attention during the last decade [7]. Recently, it was reported that the conductivity of PEDOT:PSS film is enhanced by more than 100-fold, if a liquid or solid organic compound, such as di-methyl sulfoxide (DMSO), N-N-dimethyl formamide (DMF) or tetrahydrofuran (THF), is added to the PEDOT:PSS aqueous solution [8,9]. The choice of deposition method of conducting polymers onto the conducting glass is also significant for the performance of DSSC. Different methods such as spin coating [10] and chemical polymerization [11] were employed in order to form a conductive polymer deposited counter electrode that has good electrochemical stability.

Generally, transition metal coordination compounds (ruthenium) polypyridyl complexes are used as the effective sensitizer, due to their intense charge transfer absorption in whole visible range and highly efficient metal-to-ligand charge transfer [12]. However, these complexes contain a heavy metal, which is undesirable from the point of view of the environmental aspects [13]. Moreover, the process to synthesize these complexes is complicated and costly. Alternatively, commercially available natural dyes can be used for the same purpose with an acceptable efficiency [14,15]. However, other organic dyes such as phthalocyanines, cyanine dyes, and coumarin dyes usually gave poor photovoltaic response in DSSC because of weak binding energy with TiO_2 film and low charge transfer absorption in the whole visible region range, but these dyes are very cheap and can be prepared easily, compared to ruthenium polypyridyl complexes. For example, indoline and perylene derivatives and xanthene dyes are known to be good photosensitizer [16] and have been used for DSSC [17]. The highest energy conversion efficiency achieved so far for DSSC is 10% using N719 [1], while employing metal free organic dyes it is about 8% [18].

In this study, we report the systematic investigation on the dye sensitized solar cell consisting of pyronine G (PYR) sensitized nano-structured TiO_2 on fluorine-doped tin oxide (FTO) photoelectrode, PEDOT:PSS aqueous solution coated onto a FTO as a counter electrode and an electrolyte with 0.5 ml KI and 0.05 ml iodine in acetonitride solvent. PYR dye belongs to a group of xanthane dye. These dyes have high absorption coefficients and can be easily processed and also can be functionalised to obtain the specific optical and electrical properties. This dye is used for present investigation, since this is a metal free dye and has the band gap around 1.96 eV, which is very close to that for ruthenium based dyes, which are costly in comparison to PYR dye. In addition, carbon black (0.2 wt% with respect of PEDOT:PSS aqueous solution) was added into DMSO treated PEDOT:PSS solution to enhance the conductivity. The effect of different counter electrodes on the photovoltaic response of DSSC was studied. Highest efficiency has been found in the DSSC when carbon black (0.2 wt%) DMSO treated PEDOT:PSS used as counter electrode. This may be attributed to the low charge transfer resistance and improved catalytic activity of the film due to its larger surface area. We have investigated the effect of sintering temperature and thickness of TiO_2 film, dye sensitization time and temperature of device on the photovoltaic performance for FTO/TiO_2-, PYR-electrolyte/carbon black (0.2 wt%) DMSO treated PEDOT:PSS/FTO device. Finally, the effect of TBP addition in the electrolyte on photovoltaic parameters has also been discussed in detail.

2. Experimental details

2.1. Cyclic voltammetry and optical absorption measurement

Cyclic voltammetry (CV) of the dye and dye sensitized TiO_2 was performed using a potentiostat–galvanostat (PGSTAT 30, Autolab, Eco-Chemie, Netherlands) in a three-electrode cell at room temperature. The three-electrode cell was composed of a gold working electrode, a platinum counter electrode and an SCE reference electrode, calibrated against the Fc/Fc^+ couple (+0.470 V vs. SCE). It was conducted in a distilled N,N-di-methyl formamide (DMF) solution containing 10^{-3} M of the dye and 0.1 M KCl as supporting electrolyte at a scan rate of 60 mV/s.

The optical absorption spectrum of the materials used for present investigation was recorded on Perkin Elmer UV–visible spectrophotometer. The fluorescence spectra were recorded on Hitachi fluorescence spectrophotometer.

2.2. Fabrication of symmetric devices

The configuration of symmetric device FTO/DMSO-PEDOT:PSS/electrolyte/DMSO-PEDOT:PSS/FTO is shown in Fig. 1(a) was fabricated as follows. The gap between two DMSO-PEDOT:PSS coated FTO plates electrodes was filled with a electrolyte with the concentration of iodine varying from 0.05 to 0.5 M. The active area of the symmetric devices was 1 cm^2.

2.3. Preparation of dye sensitized TiO_2 films

The conducting glass substrate (fluorine-doped tin oxide) (FTO) was cleaned and rinsed with water and 2-propanol. The FTO sub-

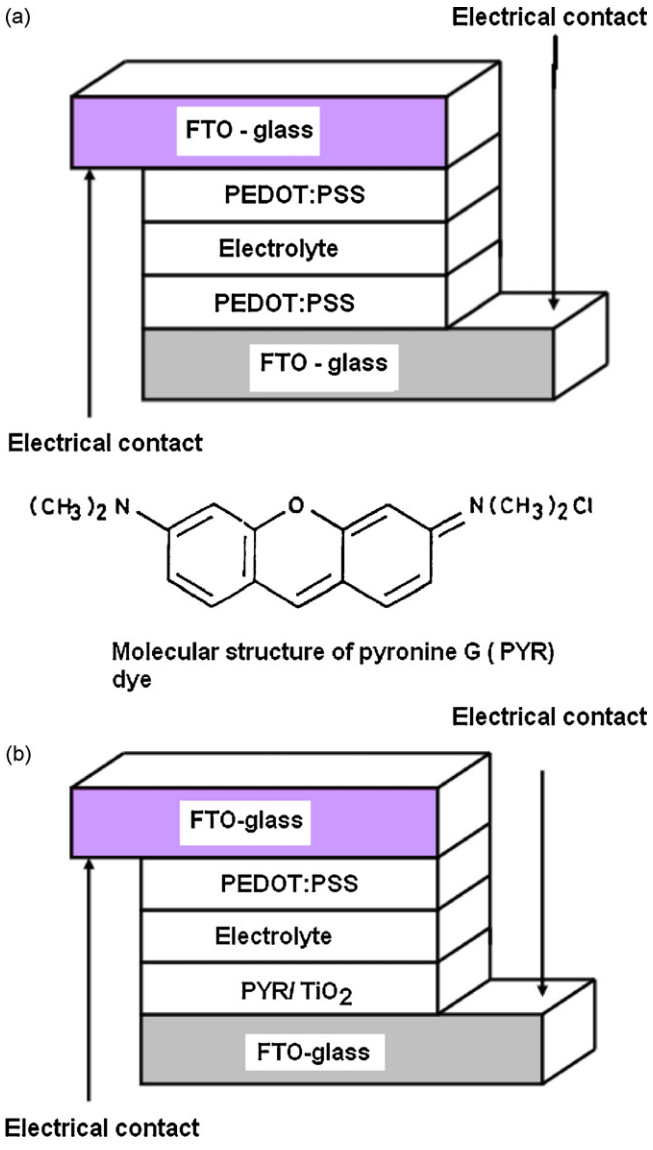

Fig. 1. (a) Schematic view of symmetric FTO/PEDOT:PSS/electrolyte/PEDOT:PSS/FTO device. (b) Schematic layout of FTO/TiO_2-PYR/electrolyte/PEDOT:PSS/FTO device along with molecular structure of pyronine G (PYR) dye.

strate was dried in vacuum prior to film preparation. The TiO_2 colloidal solution was prepared by grinding in a mortar with pestle 6 mg of TiO_2 (P25 Degussa) powder in 2 ml of distilled was water and 0.2 ml of acetylacetone, the substances were ground for 40 min. Finally 8.0 ml of distilled water and 0.1 ml of Triton X-100 were slowly added with continuous mixing for 10 min. The finely grinded paste was coated over FTO glass by doctor blade technique. After air-drying, the FTO glass coated with TiO_2 film was sintered at different temperatures, i.e. 250, 350 and 450 °C for 30 min in ambient condition and film was cooled to room temperature. A solution of 0.1 mM pyronine G (PYR) dye in DMF was used to sensitize the nano-porous TiO_2 film. The fresh nano-porous TiO_2 film was dipped into the dye solution, while its temperature was 60 °C and then kept in the solution for different sensitization times at room temperature. After sensitization, the films were washed with DMF and dried at 50 °C for 30 min.

2.4. Counter electrode preparation

Counter electrode was prepared using modified PEDOT:PSS as follows: the PEDOT:PSS aqueous solution and the organic solvent (DMSO) were mixed in the volume ratio of 3:1. The solvent-treated PEDOT:PSS film was formed on FTO by dip coating method. In order to improve the conductivity and roughness of the films, a small amount of carbon black was added with the solvent-treated PEDOT:PSS aqueous solution. The film was dried at 80 °C for 30 min in air.

2.5. DSSC assembling and measurement

The two electrode sandwich cell for photovoltaic measurements consisted of a dye sensitized TiO_2 FTO photoelectrode, a organic electrolyte containing tri-iodide and iodide and a PEDOT:PSS coated FTO electrode. The counter electrode and dye sensitized TiO_2 electrode were clamped firmly together and redox electrolyte typical of 0.5 M KI/0.05 M I_2 in acetonitrile solution was introduced into the porous structure of the dye sensitized TiO_2 electrode by capillary action. The cross-sectional view of the DSSC is shown in Fig. 1(b). The photovoltaic performance of the DSSCs was recorded with HP semiconductor analyzer. A 100 W halogen lamp was used as light source. The intensity of the illumination light is 100 mW/cm^2. The dark current measurement of the devices was conducted in a dark box with same instrument.

The flat band potential of devices was measured by the Mott–Schottky analysis method [19,20]. The Mott–Schottky analysis was performed on potentiostat (PGSTAT 30, Autolab, Eco-Chemie, Netherlands) with frequency response analyzer (FRA) in the potential range from 0 to −1.5 V.

3. Results and discussion

In dye sensitized solar cell (DSSC), the iodide in the electrolyte regenerates the positively charged photo-excited dye by electron donations, i.e.

$$3I^- + (2dye)^+ \rightarrow 2dye + I_3^-$$

The tri-iodide is reduced back to iodide at the counter electrode, i.e.

$$I_3^- + 2e^- \rightarrow 3I^-$$

Therefore, the diffusion of iodide and especially of tri-iodide in the electrolyte as well as the charge transfer at the counter electrode/electrolyte interface is an important parameter that influences the performance of the DSSC. Therefore, we have investigated the charge transfer mechanism in symmetric device using different counter electrodes.

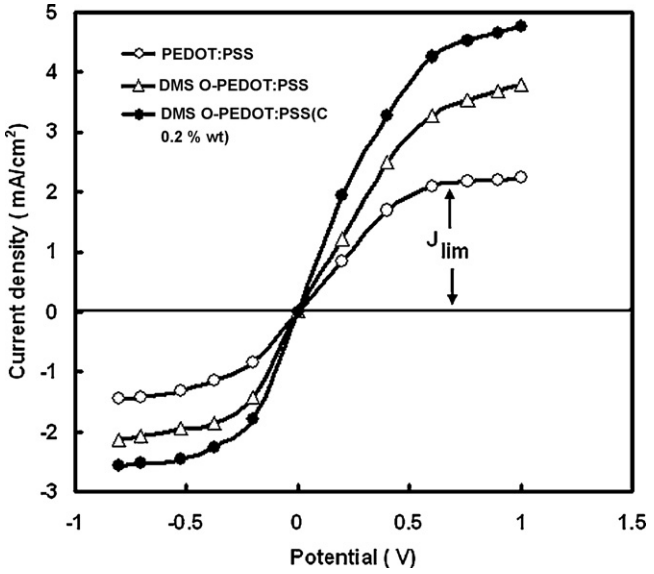

Fig. 2. Cyclic voltammogram of symmetric devices using different counter electrodes.

3.1. Symmetric cells

We have recorded the cyclic voltammetry of symmetric device using different counter electrodes, i.e. PEDOT:PSS, DMSO treated PEDOT:PSS (DMSO-PEDOT:PSS) and carbon black (0.2 wt%) DMSO treated PEDOT:PSS (DMSO-PEDOT:PSS (*C* 0.2 wt%) and shown in Fig. 2. The saturation in current density denotes the limited current density (J_{lim}). The relationship between the diffusion coefficient and the limited current is described as follows [21]

$$J_{lim} = \frac{2nqD_{I_3^-}C_{I_3^-}N_A}{l} \quad (1)$$

where n denotes the number of electron transferred in the reaction (here $n = 2$), q the elementary charge, $D_{I_3^-}$ the diffusion coefficient of I_3^-, $C_{I_3^-}$ concentration of I_3^-, N_A the Avogadro constant and l denotes the distance between the electrodes. It can be seen from Fig. 2, the limited current (J_{lim}) is more for the treated PEDOT:PSS electrodes than untreated electrodes indicates the enhanced electroactivity for this electrode [22].

We have recorded the cyclic voltammogram (CV) of the symmetric devices at different temperatures and the J_{lim} and diffusion coefficient were obtained from CV response at different temperatures and shown in Fig. 3 for symmetric cell with DMSO-PEDOT:PSS (*C* 0.2 wt%) used as counter electrode. According to Arrhenius's law, the diffusion coefficient exponentially varies with temperature as described in Eq. (2) [23], therefore an exponential increase of J_{lim} with increasing temperature is also expected as shown in Fig. 3.

$$D = D_0 e^{-E_a/RT} \quad (2)$$

where D denotes the diffusion coefficient, D_0 is the temperature independent pre-exponential, E_a is the activation energy, R is the gas constant and T denotes the absolute temperature. Similar results have been obtained for other symmetrical devices employing other counter electrodes. It is found that the activation energy extracted from these data are 3.4, 2.3 and 1.7 J/mol for devices using PEDOT:PSS, DMSO-PEDOT:PSS and DMSO-PEDOT:PSS containing carbon black coated thin film over ITO as counter electrodes. This indicates that the low value of activation energy also have impact on the device performance.

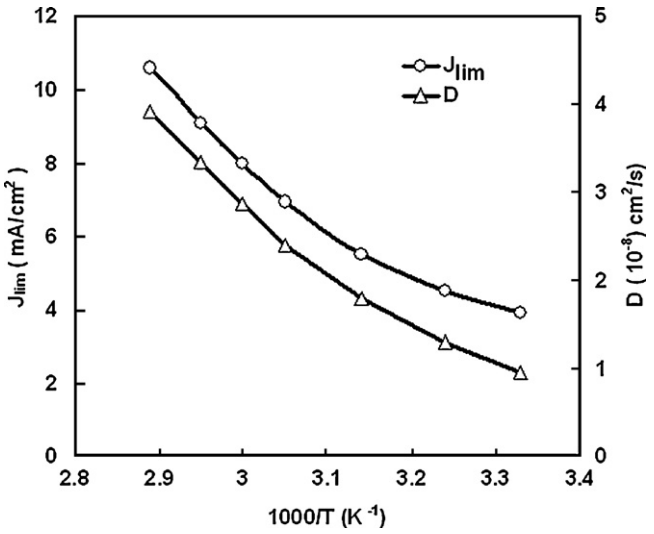

Fig. 3. Variation of limited current density (J_{lim}) and diffusion coefficient (D) with temperature for symmetrical device with DMSO-PEDOT:PSS (C 0.2 wt%) counter electrode.

Another important parameter is the charge transfer resistance (R_{ct}) that acts as a barrier for electrons reducing tri-iodide to iodine. The 2 R_{ct} of two interfaces with electrolyte have been determined from the impedance spectrum of the symmetric cells measured in the frequency range 1 Hz to 1 MHz and shown in Fig. 4 for ITO/PEDOT:PSS/electrolyte/PEDOT:PSS/ITO device. Similar results have been obtained for other devices fabricated with DMSO-PEDOT:PSS and DMSO-PEDOT:PSS (C 0.2 wt%) counter electrodes. 2 R_{ct} is taken as the impedance difference when the phase become zero in the high and low frequency regime as shown in Fig. 4. The values of charge transfer resistance (R_{ct}) for the devices are 23.5, 15.6 and 11.4 Ω for PEDOT:PSS, DMSO-PEDOT:PSS and DMSO-PEDOT:PSS (C 0.2 wt%) coated ITO counter electrodes, respectively. This indicates the counter electrode DMSO-PEDOT:PSS thin film containing carbon black has lower charge transfer resistance, can efficiently induce the reduction of I_3^- to I^- in the electrolyte. The above results show that both the activation energy and charge transfer resistance will be responsible for the photovoltaic performance of the DSSC as discussed in the later part of discussion.

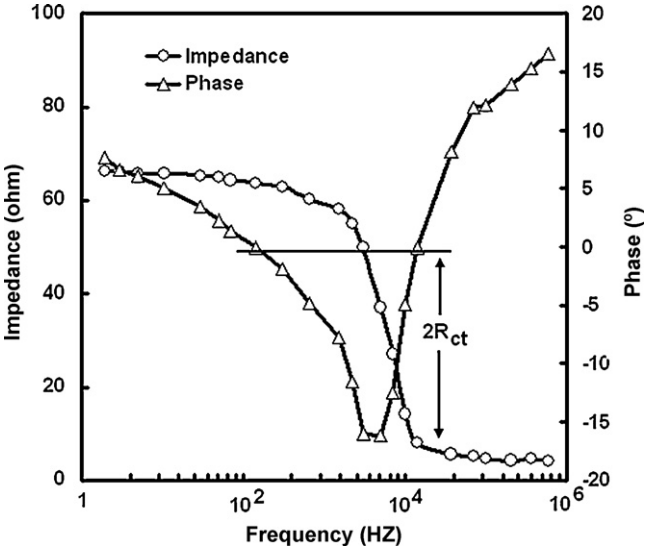

Fig. 4. Impedance spectra of FTO/PEDOT:PSS/electrolyte device at room temperature.

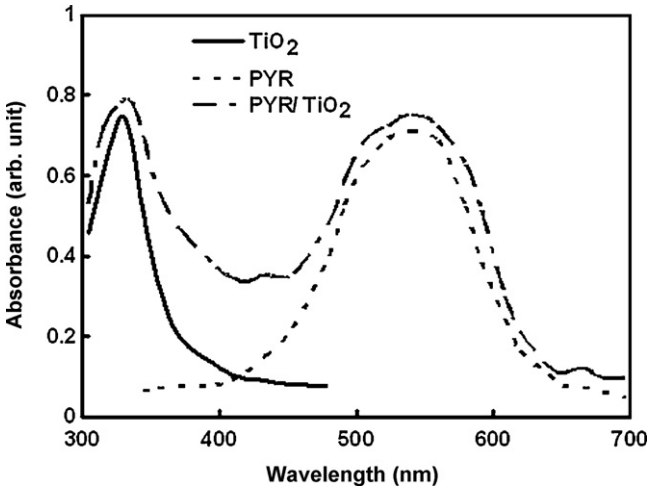

Fig. 5. Optical absorption spectra of TiO_2, PYR and PYR-TiO_2 thin films.

3.2. Dye sensitized solar cells

3.2.1. Optical and electrochemical properties

We have used PYR dye as sensitizer, whose chemical name is N-(6-(dimethylamino)-3-xanthane-3-ylidene)-N-methyl methanaminium ion. The molecular structure of PY dye has been already shown in Fig. 1(b). In Fig. 5, the typical UV–vis absorption spectra of TiO_2, PYR and TiO_2/PYR in thin film form are shown. The molecular system of the PYR (Fig. 1(b)) shows the phenomena of extended conjugation which in fact is responsible for its absorption in the longer wavelength side, i.e. absorption peak and edge around at 540and 640 nm, respectively. The absorption peak of PYR at 540 nm, ascribed to the $\pi \rightarrow \pi^*$ transition of the conjugated dye. The spectrum of the TiO_2/PYR is apparently formed of two components contribution and no wavelength shift with respect to PYR is observed, thus indicating a negligible ground state charge transfer at the interface formed between TiO_2 and PYR [24]. In Fig. 6(a) and (b), the fluorescence (FL) spectra of pure PYR and that of its mixture with TiO_2 nano-crystals in solution and film, respectively, were shown. The emission feature of the PYR is not affected by the presence of TiO_2 nano-crystals, however, slight quenching of the fluorescence intensity has been observed in solution. A remarkable quenching in the fluorescence intensity has been observed, when the fluorescence spectra recorded in thin film form as shown in Fig. 6(b). The fluorescence quenching in the presence of TiO_2 nano-crystals can be attributed to either energy or charge transfer from PYR to the inorganic semiconductor. Although a Forster energy transfer mechanism has been invoked for CdSe, InP and PbS nanocrystals embedded in conjugated polymers [25,26]. Since, we have not observed any overlapping between the TiO_2 absorption and PYR emission spectrum, the above energy transfer mechanism is not accounted for the present system. Consequently, the transfer of photogenerated electrons from PYR to TiO_2 conduction band should be responsible for PYR emission quenching as shown in Fig. 6(a) and (b). In the present system, the charge separation and transfer processes took place at the interface with the PYR, irrespective of the organic capping on the TiO_2 surface.

Fig. 7(a) shows the cyclic voltammetric behavior of PYR film deposited on ITO substrate. The reduction of PYR shows a quasi-reversible electrochemical doping/de-doping process, while the PYR oxidation (p-doping) is characterized by a quasi-reversible electrochemical response. The energy band gap of the PYR ($E_g = q\Delta\phi$) has been estimated from the difference between the energies of the lowest unoccupied molecular orbital (LUMO) and highest occupied molecular orbital (HOMO) levels, which can

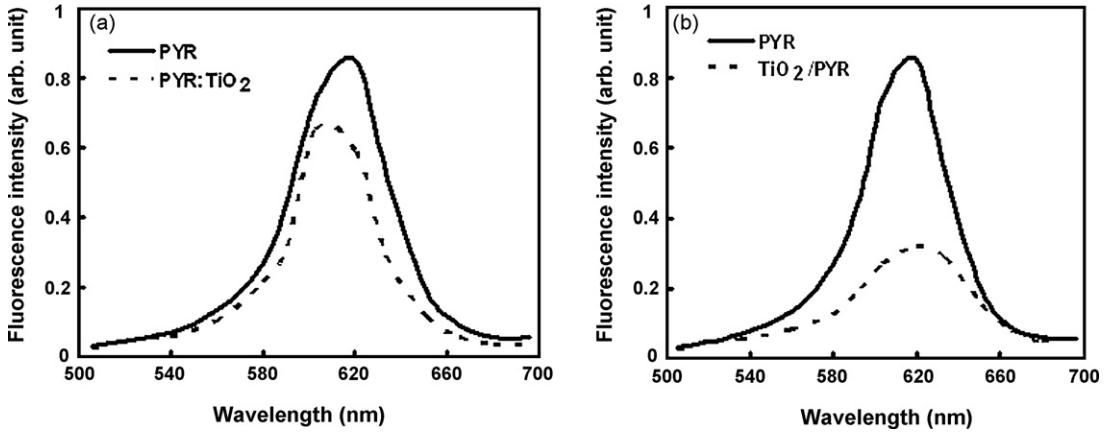

Fig. 6. (a) Fluorescence spectra of (a) PYR and PYR-TiO_2 in (a) solution and (b) thin film.

be evaluated from the onset potential of the *n*-doping (ϕ_n) and *p*-doping (ϕ_p) processes, respectively. The energy levels can be estimated with respect to saturated calomel electrode (SCE) as reference electrode by adding 4.4 eV to the corresponding measured electrochemical potentials [27], using following expressions.

$$E_{LUMO} = -q(\phi_n + 4.4) \quad (3a)$$

and

$$E_{HOMO} = -q(\phi_p + 4.4) \quad (3b)$$

The estimated value of energy band gap (E_g) is quite close to that extrapolated from the absorption onset, i.e. the optical energy band gap (1.96 eV). In Fig. 7(b), the cathodic current/potential behavior of TiO_2 nano-crystalline electrode is shown. In Fig. 8(a) and (b), the *n*- and *p*-doping processes for PYR sensitized TiO_2 electrode are displayed. In the reduction cycle, the PYR sensitized TiO_2 electrode exhibits *n*-doping and *n*-de-doping peak shifted to higher potentials with respect to those found for pure PYR. In oxidation cycle, only an irreversible *p*-doping is observed, appearing shifted to higher potential as compared with that for pure PYR. The shift to higher potentials of both the *n*- and *p*-doping curves suggests a lower ionic conductivity of the PYR/TiO_2 film than PYR. The lower oxidation current can be attributed to a decrease in the *p*-type conductivity of the PYR by the presence of the TiO_2.

3.2.2. Effect of counter electrode on photovoltaic response

We have prepared three different DSSCs using different modified counter electrode to get insight into the effect of counter electrode in photovoltaic performances of the DSSCs. Fig. 9 shows the incident monochromatic photon to electron conversion efficiency (IPCE) as a function of the wavelength of the incident light, which is defined as the number of electrons generated by light in the external circuit divided by the number of incident photons and is calculated using the following equation [28].

$$\text{IPCE}(\%) = \frac{1240 J_{sc}(\mu A/cm^2)}{\lambda(nm) P_{in}(W/m^2)} \quad (4)$$

where J_{sc} is the short circuit photocurrent density, λ is the excitation wavelength, and P_{in} is the incident light intensity. All the devices exhibit photoelectric activities over their whole absorption bands (Fig. 5), indicative of the participation of the excited state (S^*) in the electron injection process. The IPCE at a wavelength is the production of three efficiencies [29,30], i.e. IPCE = LHE (λ) × Φ_{in} × Φ_c, in which LHE (λ) is the light harvesting efficiency at a wavelength of λ, Φ_{in} is the electron injection efficiency and Φ_c is the collection efficiency of the injected electrons at the back contact of the photoanode. Φ_c is associated with (i) the electron transport within the TiO_2 network, (ii) the recombination of the injected electrons with the electrolyte (I_3^-), and (iii) the recombination of the injected electrons with the oxidized dye and therefore should be independent of excitation wavelength. Since we have used different counter electrodes having same configuration, the improvement in IPCE for DMSO treated PEDOT:PSS is due to only increased conductivity of counter electrode. As we have already discussed in Section 3.1 that the charge transfer resistance (R_{ct}) depends on the reduction of I_3^- into I^- in the electrolyte. It is observed that the charge transfer resistance is highest and lowest for PEDOT:PSS and DMSO-PEDOT:PSS containing carbon black counter electrodes, respectively. This lower

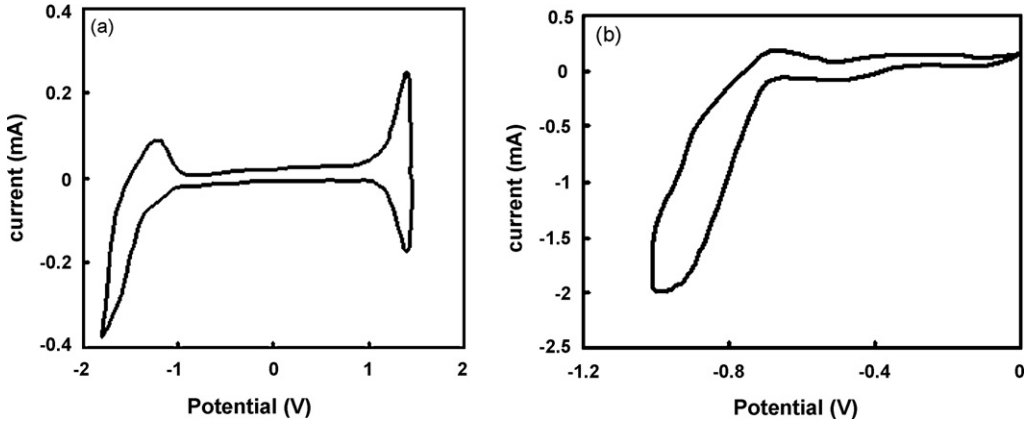

Fig. 7. Cyclic voltammetry (reduction and oxidation cyclic) of (a) PYR and (b) TiO_2 thin films.

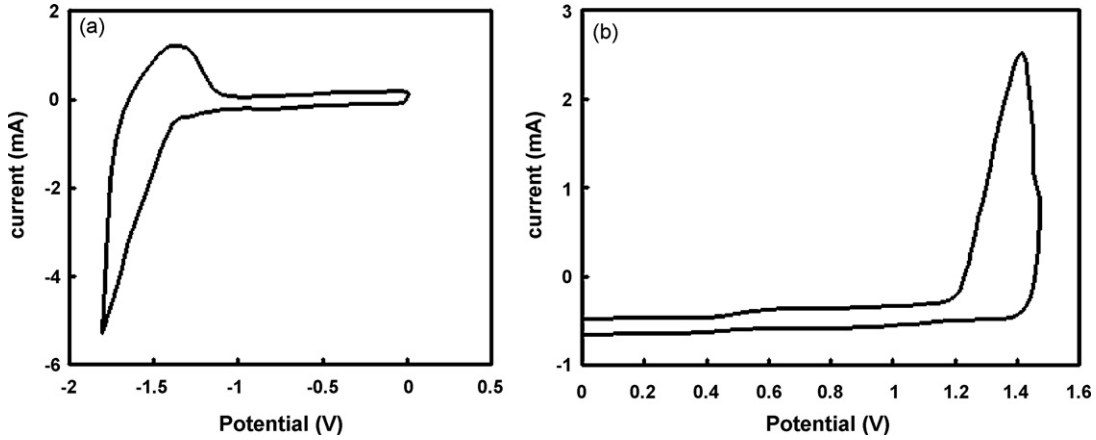

Fig. 8. Cyclic voltammetry of PYR sensitized TiO_2 electrode (a) reduction (b) oxidation.

value of charge transfer resistance indicates that the more sites are available for reducing I_3^- to for I^- in the electrolyte for dye sensitized solar cell with DMSO-PEDOT:PSS containing carbon black as counter electrode than other counter electrodes, responsible for the increase in IPCE.

Fig. 10 shows the photocurrent–photovoltage characteristics of the DSSCs with different counter electrodes made of PEDOT:PSS, DMSO-PEDOT:PSS and DMSO-PEDOT:PSS (*C* 0.2 wt%). Table 1 summarizes the performance of data of all devices under the illumination of intensity 100 mw/cm^2. For a DSSC containing the PEDOT:PSS counter electrode, it is seen from the table that the photovoltaic characteristics, including the short circuit current density (J_{sc}), the open circuit voltage (V_{oc}), the fill factor (FF) and power conversion efficiency (η) are improved, when PEDOT:PSS is treated with DMSO. The *J–V* characteristics were dramatically improved, and the conversion efficiency of DSSC made of a DMSO. The photovoltaic parameters are further enhanced when the suitable amount (0.2 wt%) of carbon black was added to the DMSO treated PEDOT:PSS. This indicates that the DMSO play a role of enhancing conductivity of the PEDOT:PSS film. Moreover, carbon black plays an important role in further increasing the catalytic activity of the film due to its large surfaces area. This indicates that the charge transport of the redox couple in the electrolyte and charge transfer at the counter electrode/electrolyte interface have been improved for the DSSC with DMSO-PEDOT:PSS (*C* 0.2 wt%) counter electrode. This also indicates the counter electrode DMSO-PEDOT:PSS thin film containing carbon black has lower charge transfer resistance, can efficiently induce the reduction of I_3^- to I^- in the electrolyte.

3.2.3. *Effect of dye sensitization time, thickness and sintering temperature of TiO_2 layer*

A requirement for the dye structure is that it should possess several =O or –OH groups capable of anchoring to the Ti (IV) sites on the TiO_2 surface. The molecular structure of pyronine G (PYR) dye shown in Fig. 1(b), exhibits the =O group, which is responsible for the transferring of excited electrons into TiO_2. Since the DSSC having the carbon black added (0.2 wt%) DMSO treated PEDOT:PSS coated FTO substrate gives the highest power conversion efficiency, we have carried the further investigation only on this device. The effect of dye sensitizing time on the IPCE action spectra is shown in Fig. 11. The dye sensitization has been achieved by immersing the nano-structured electrode into a PYR dye solution in DMF. The following processes may describe the dye sensitization into TiO_2: (i) diffusion of dye into TiO_2 nano-structured, (ii) adsorption of the dye to the TiO_2 surface, and (iii) dissolution of Ti surface atoms from TiO_2 and formation of Ti^{2+}/PYR complex in the pores of the TiO_2 film. Depending upon the rate of these different processes, the outer part of the electrode form Ti^{2+}/PYR complexes in the pores, when dye molecules reach, the interface between the bulk contact and the TiO_2 film. Therefore, the latter process increases the efficiency, whereas the former is responsible for the decrease in the efficiency. The results in Fig. 11 are consistent with such phenom-

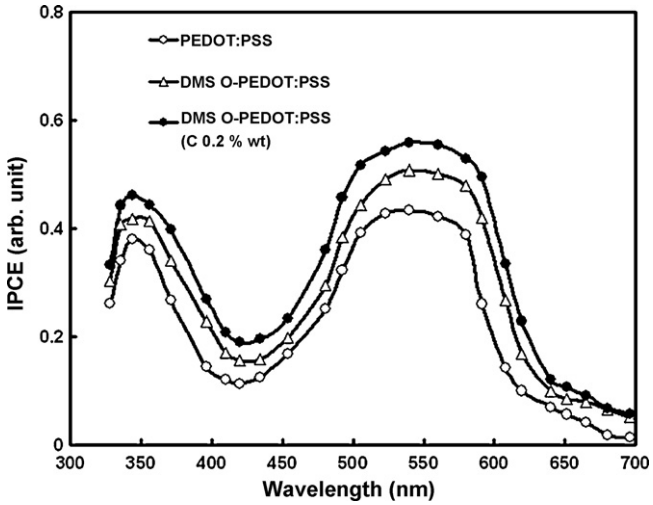

Fig. 9. IPCE spectra of DSSC using modified PEDOT:PSS counter electrodes.

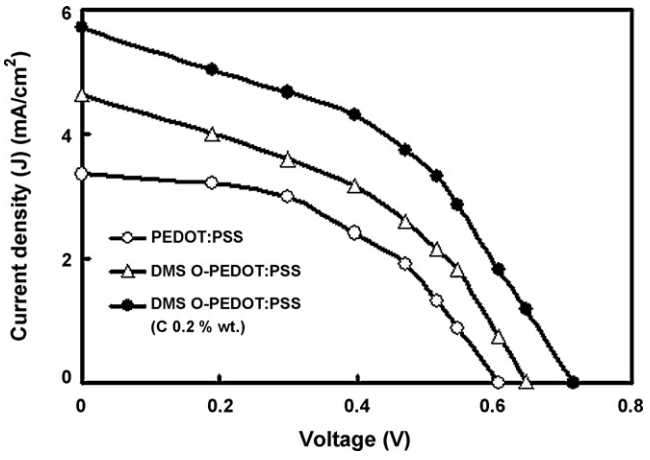

Fig. 10. Current–voltage characteristics of DSSC under 10 mW/cm^2 illumination with different PEDOT:PSS counter electrodes.

Table 1
The performance of the DSSC with different counter electrodes used including PEDOT:PSS, DMSO treated PEDOT:PSS and DMSO treated PEDOT:PSS with carbon black contents.

Counter electrodes	Short circuit Current (J_{sc}) (mA/cm^2)	Open circuit voltage (V_{oc}) (V)	Fill factor	Power conversion efficiency (η) (%)
PEDOT:PSS	3.36	0.60	0.52	1.06
DMSO-PEDOT:PSS	4.1	0.65	0.55	1.46
DMSO-PEDOT:PSS (*C* 0.2 wt%)	5.7	0.72	0.58	2.38

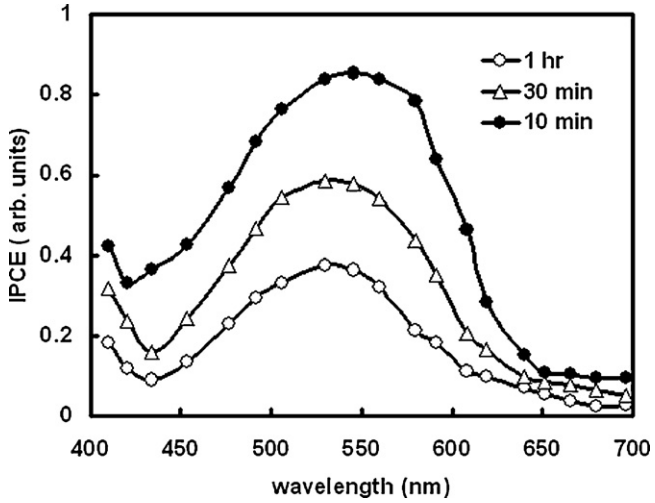

Fig. 11. Effect of dye sensitization time on IPCE spectra.

ena. The IPCE and short circuit photocurrent decreases with longer time of sensitization time. The results indicate that protons from dyes causes the dissolution of Ti surface atoms and formation of Ti^{2+}/PYR complex in the pores of the nano-structured film, which gives rise to a filter effect (inactive molecules).

The effect of sintering temperature of TiO_2 film on the performance of DSSCs consist of the structure ITO/TiO_2/PYR/electrolyte/DMSO treated PEDOT:PSS/ITO was also been investigated. Fig. 12 shows the photocurrent–photovoltage curves nano-structured TiO_2 films sintered at 250, 350 and 450 °C. These curves clearly show that the sintering of TiO_2 nano-structured TiO_2 film at high temperatures results high photocurrent and high power conversion efficiency. The thickness of film is 8.0, 6.2 and 4.5 μm, when fabricated at 250, 350 and 450 °C, respectively. It is also observed that the thickness of film is large although these films were fabricated by doctor blade method already mentioned. However, the

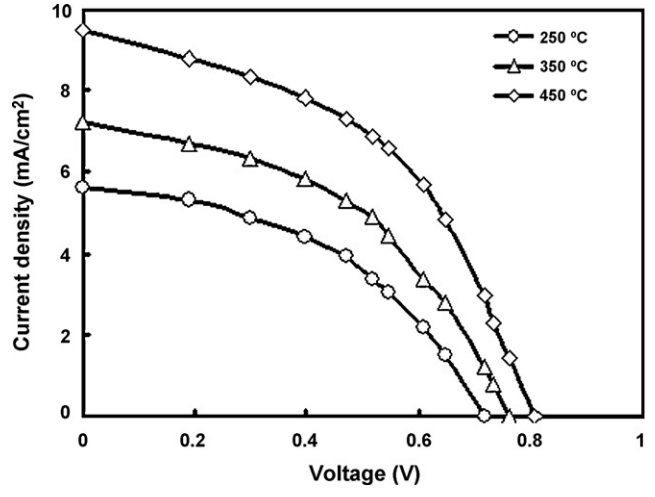

Fig. 12. Photocurrent–photovoltage characteristics of FTO/TiO_2-dye/electrolyte/DMSO-PEDOT:PSS (*C* 0.2 wt%) FTO device.

DSSC consisting of TiO_2 nano-structured thin film sintered at higher temperature results higher power conversion efficiency. We have mentioned that such a film can absorb smaller amount of dye than that formed at low temperature, indicating that the film structure play a key role in DSSC. Zukalova et al. [31] have also reported that the performance of DSSCs fabricated with organized TiO_2 mesoporous film is improved, if the crystallinity of the TiO_2 film is enhanced by high sintering temperature. The increasing temperature leads to the formation of high crystallinity film, which improve the network structure of the film and enhances the interconnection between particles resulting in swift diffusion of electrolyte and good transport electrons in the film [32].

We have investigated the effect of the thickness of TiO_2 layer sintered at 450 °C in electrode, on the DSSC current–voltage characteristics. The variation of short circuit photocurrent (J_{sc}), open circuit voltage (V_{oc}), fill factor (FF) and power conversion efficiency (η) are presented in Fig. 13(a) and (b). These results show that as the thickness of electrode increases, J_{sc} first increases abruptly, reaches to its peak value and gradually decreases afterwards. Such variation in J_{sc} can be explained by electron photogeneration. For a given porosity and pore size, an increase in electrode thickness directly increases internal surface area, resulting in a higher dye loading. Therefore, thicker electrode can absorb more photons, leading to a higher J_{sc}. However, if the electrode thickness is greater than the light penetration depth, the number of photons useful for electron photogeneration will reach the limit and, therefore, J_{sc} cannot be increased any further. Instead, an increase in the thickness beyond the light penetration depth yields more recombination centers that cause a higher electron loss and thus a gradual reduction in J_{sc}. Fig. 13 also shows that V_{oc} decreases with increasing electrode thickness. This phenomenon can be explained by the electron dilution effect [33]. As the light is transmitted into the depth of an electrode, the light intensity gradually decreases. Therefore, as thickness increases, the excessive electron density becomes lower resulting in a lower V_{oc}. The higher series resistance of a thicker electrode also contributes to the reduction in photovoltage. The decrease in V_{oc} can also be attributed to the increased charge recombination and restricted mass transport in thicker films [33,34]. The fill factor was found to decrease with increasing electrode thickness indicating an increase in internal resistance of the device.

We have investigated the effect of temperature on the photovoltaic performance. It is observed that when the temperature of the device increases from room temperature to 80 °C, V_{oc} decreases from 0.79 to 0.71 V, while the J_{sc} rises from 8.5 to 10.6 mA/cm^2. The fill factor shows practically no change with temperature for the device. The observed decrease in V_{oc} attributed to the increase in dark current with the increase in temperature. An increased dark current implies a higher value for the rate constant of tri-iodide reduction, which accordingly leads to a lower value of V_{oc}.

$$V_{oc} = \left(kT/q\right)\left[\ln\left(\frac{I_{inj}}{n_{cb}k_{et}[I_3^-]}\right)\right] \quad (5)$$

where I_{inj} is the flux of charge resulting from sensitized injection and n_{cb} is the concentration of electrons in the conduction band of TiO_2.

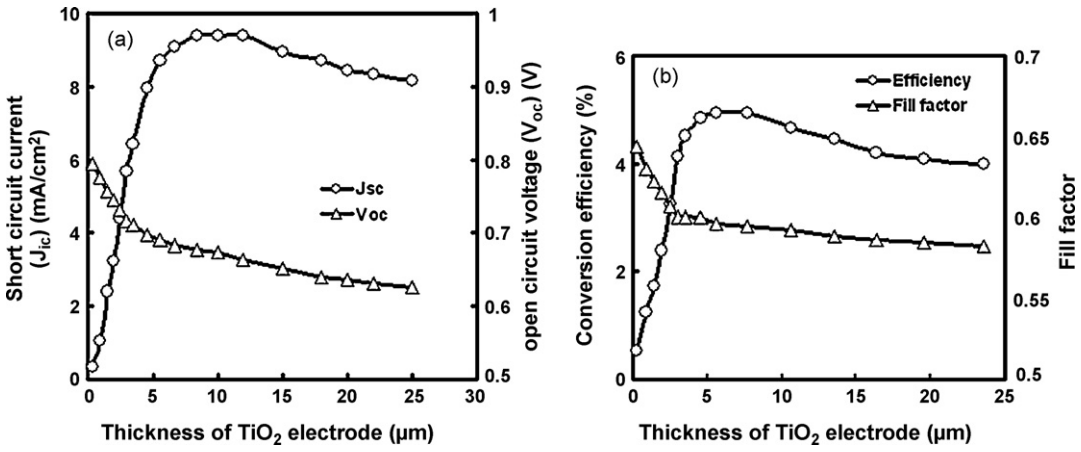

Fig. 13. (a) Effect of TiO_2 thickness on (a) short circuit current and open circuit voltage, (b) power conversion efficiency and fill factor of DSSC.

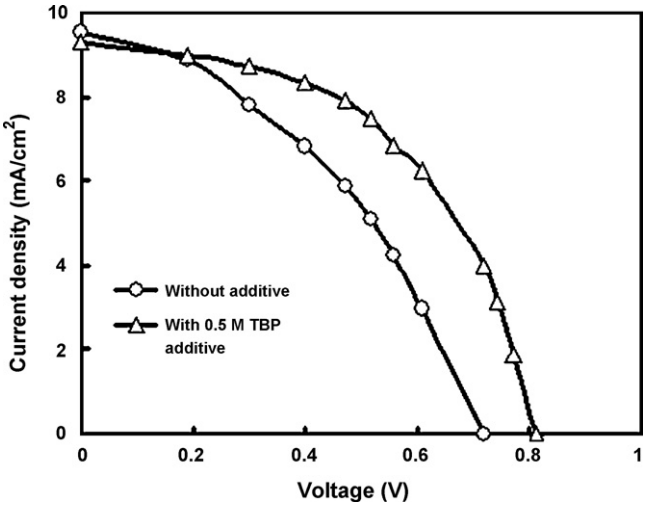

Fig. 14. Effect of TBP addition in liquid electrolyte on current–voltage characteristics under the illumination of DSSC.

3.2.4. Effect of TBP addition in the electrolyte

Fig. 14 refers to the effect of 4-tert-butyl pyridine (TBP) additives in the liquid electrolyte on the current–voltage characteristics under the illumination of DSSC based on optimized TiO_2 thickness sintered at 450 °C. The values of photovoltaic parameters are shown in Table 2 for different concentration of TBP in the liquid electrolyte. The addition of TBP in the liquid electrolyte improves the fill factor and V_{oc} of the device significantly, without affecting the J_{sc}. The increase in the V_{oc} and FF by TBP is due to the suppression of the dark current at TiO_2/electrolyte junction. The dark current arises from the reduction of tri-iodide by conduction band electrons.

$$I_3^- + 2e_{cb}^- TiO_2 \rightarrow 3I^-$$

Which occurs despite of that the TiO_2 surface is covered by a layer of PYR dye. The tri-iodide, due to its relatively smaller size, either crosses the dye layer or has access to nanometer sized pores into which dye cannot penetrate, i.e. where the surface of TiO_2 is bare and exposed to redox electrolyte. The effect of TBP is to decrease the rate of the reduction of tri-iodide. It is observed that the onset of dark current is shifted by 0.2 V, when TBP is added into the electrolyte. The decrease in the rate constants for tri-iodide reduction (k_{et}) should lead to an increase in the V_{oc} of the device. The open circuit voltage of the DSSC is thermodynamically determined by the difference between the electron quasi-Fermi level in the TiO_2 film under illumination and the redox potential of the redox couple in the electrolyte [35,36]. In dynamic processes, two possible factors influence the V_{oc} [37]. One is the change in the charge recombination at the TiO_2 electrode/redox electrolyte interfaces, and the other is the band edge shift of TiO_2 with respect to the redox potential to the electrolyte.

We evaluated the flat band potential V_{fb} of TiO_2 electrode in different electrolytes using the Mott–Schottky analysis method [19,20]. We have estimated the differential capacitance from the impedance analysis of the devices at different applied potential. The relationship between the capacitance and applied potential can be expressed by the following equation

$$\frac{1}{(C_{sc})^2} = \frac{2\left(\left|V - V_{fb}\right| - (kT/q)\right)}{\varepsilon\varepsilon_o q N_d} \quad (6)$$

where C_{sc} is the space charge capacitance, ε is the dielectric constant for semiconductor, ε_o is the permittivity of free space. N_d is the dopant density, V_{fb} is the flat band potential and V is the applied voltage. Fig. 15 shows the typical Mott–Schottky curves versus applied potential for TiO_2 film in the electrolyte containing different concentration of TBP. The inset shows the plot for the TiO_2 film in the electrolyte without TBP. The plot $1/(C_{sc})^2$ versus the applied potential shows x-intercept corresponding to V_{fb}. The deviation from linearity may result from the effect of surface states, recombination effects and non-negligible contributions of the Hemholtz layer to the interfacial capacitance [38]. Table 3 summaries the effects of TBP on V_{fb}. It is observed that the addition of TBP additives to the electrolyte, V_{fb} shifted to a more negative value. A higher concentration of TBP additives gives rise to a more negative potential.

There was a dramatic improvement on V_{oc} after the TBP was added into electrolyte as shown in Table 2. One of the possible explanations for the improvement of V_{oc} can be related to the

Table 2
Effect of TBP additives on the photovoltaic properties of DSSC using TiO_2 sintered at 450 °C.

Additives	Short circuit Current (J_{sc}) (mA/cm²)	Open circuit voltage (V_{oc}) (V)	Fill factor	Power conversion efficiency (η) (%)
None	9.5	0.72	0.64	4.58
0.1 M TBP	9.38	0.78	0.67	4.88
0.5 M TBP	9.27	0.82	0.69	5.24

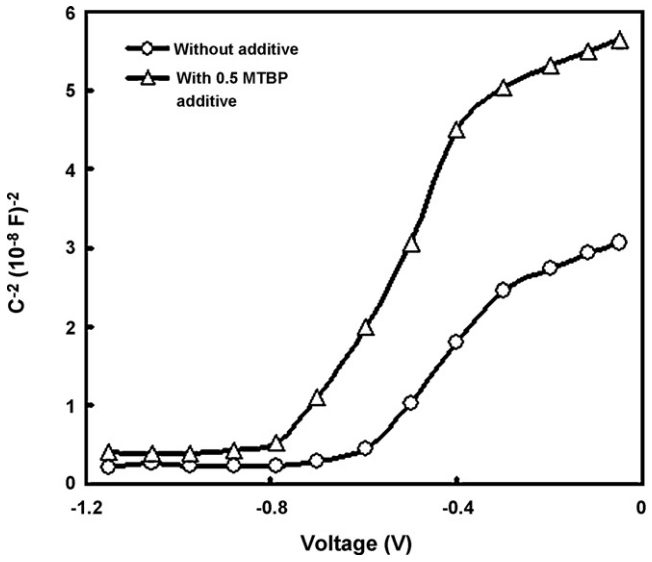

Fig. 15. Mott–Schottky curves ($1/C^2$–V) for the DSSC.

negative shift of V_{fb} of the TiO_2 electrolyte in the different electrolytes. It can be seen from the Table 3 that the ΔV_{oc} was smaller than the corresponding ΔV_{fb} for TBP additives. In addition, another factor to affect the V_{oc} is the back electron transfer at the electrode/dye/electrolyte interfaces. According to the Marcus–Gericher theory [39], the interfacial transfer rate constant from the conduction band of the redox species in the electrolyte is expressed by the following equation

$$k_{et} = \delta \nu_{th} \sigma \left[\frac{kT}{\pi\lambda}\right]^{1/2} \exp\left(-\frac{(E_{redox} - \lambda - E_{cb})^2}{4\lambda kT}\right) \quad (7)$$

where δ is the reaction layer thickness for interfacial electron transfer, ν_{th} is the thermal velocity of the electron, σ is the reaction cross-section and λ is the solvent reorganization energy. When conduction band of TiO_2 shifts negatively, the driving force increases for the charge recombination from the conduction to the redox in electrolyte, resulting in the enhancement of the rate of back electron transfer and thus the decrease of open circuit voltage (V_{oc}). Frank and coworkers [40] have also reported that with the addition of some additives such as ammonia in the electrolyte, caused the band to move negatively and recombination to increase, the effect of which was to improve V_{oc}. Therefore, we believe that the ΔV_{oc} was smaller than ΔV_{fb}, which is in part due to the enhancement of back electron transfer after the addition of TBP in electrolyte. Gratzel and coworkers [28] have also reported that adsorption of 4-TBP at the TiO_2 surface is caused by interaction between the Ti (IV) ion, which has Lewis acidity, and the lone electron pair of 4-TBP. Therefore, the larger the partial charge on the nitrogen or oxygen atom of the pyridine derivatives additives is, the easier and the more often the pyridine derivatives can be adsorbed onto the Lewis acid sites of the bare TiO_2 surface, which would cause a larger V_{oc} by negative shifting of the conduction band edge of TiO_2 [41]. For higher concentration of TBP, more pyridine could be easily adsorbed onto the Lewis acid site of TiO_2, which led to the fast rate of back electron transfer. Under illumination, the dye adsorbed on the TiO_2 nano-particles inject electrons into the conduction band, and the conduction band edge of the TiO_2 electrode dramatically shifts towards negative, especially after TBP was added [42]. The negative shift of the conduction band enhances the driving force for the recombination at the interface between I_3^-/I^- in the electrolyte, leading to a decrease of V_{oc} according to the Marcus–Gericher theory. However, V_{oc} is enhanced after the addition of TBP as shown in table.

Table 3
Flat band potential of TiO_2 (V_{fb}) and changes in V_{fb} (ΔV_{fb}) and V_{oc} (ΔV_{oc}) of DSSC before and after the addition of TBP in electrolyte.

Additives	Flat band potential (V_{fb}) (V)	ΔV_{fb} (V)	ΔV_{oc} (V)
None	−0.68	0.0	0.00
0.1 M TBP	−0.73	−0.05	0.06
0.5 M TBP	−0.83	−0.15	0.1

The dark current in DSSC arises from the reduction of tri-iodide by the conduction band electrons [28]. We have recorded the J–V characteristics of the devices in dark and observed that the dark current was reduced after the addition of TBP in the electrolyte. The small dark current leads to a large open circuit voltage [28,43]. With the addition of TBP additives, we assume that the distance between the TiO_2 and I_3^- increases [44]. The dark current is a qualitative measure of interface charge recombination at the dye sensitized TiO_2 in DSSCs. The results of dark current strongly support the conclusion that the negative shift of the conduction band edge of TiO_2 is the predominant factor determining the V_{oc}.

In the case of open circuit conditions, the absolute value of the recombination current density J_{recomb} equals the absolute value of the current density of photogenerated electrons J_{inj}, i.e. $J_{recomb} = J_{inj}$. Since, the electron concentration in dark is negligible, it holds that $J_{recomb} = n_t q k_{et} C_{ox} n$, where n_t being the number of electrons involved in the charge transfer process to the oxidized species of concentration C_{ox} with the transfer rate k_{et} and q is the electronic charge. The electron density n can be approximated by an exponential dependence on photovoltage V.

$$n = N_C \exp\left[-\frac{E_{ref} - eV}{kT}\right] \quad (8)$$

where N_C is the effective density of states in the conduction band and the reference energy E_{ref} being the difference between the conduction band edge energy E_c and the redox potential of the active redox couple E_{redox}, $E_{ref} = E_C - E_{redox}$. This leads to [45]

$$J_{recomb} = q n_t k_{et} C_{ox} N_C \exp\left[-\frac{E_{ref} - qV}{kT}\right] \quad (9)$$

The open circuit voltage can be expressed as [35]

$$V_{oc} = \left(\frac{kT}{q}\right) \ln\left[\frac{J_{inj}}{q n_t k_{et} C_{ox} N_C}\right] + \frac{E_C - E_{redox}}{q} \quad (10)$$

Within the limits of its approximation, the above equation leads to the interpretation that the open circuit voltage is determined, on one hand, by a constant contribution given by difference between the semiconductor's conduction band edge and the redox potential of the redox active species in the electrolyte. On the other hand, V_{oc} is reduced by the recombination of charge carriers at the TiO_2/electrolyte interface i.e. when the recombination rate is high then V_{oc} will be low. The above equation therefore suggests temperature dependent measurements of photocurrent–voltage as an ideal tool to differentiate between effects related to band edge movement and the influence of a change recombination rate. Fig. 16 shows the variation of open circuit voltage as a function of temperature both for a device treated with TBP as well as for untreated device. The device consisting of untreated electrolyte shows not only the overall lower values of V_{oc} but also a stronger dependence of V_{oc} on temperature. According to Eq. (10), this implies a higher recombination rate for the device without TBP treatment. The increase in V_{oc} with the addition of TBP in the electrolyte may also be ascribed by the adsorption of TBP on the TiO_2 surface, which is responsible for the reduced recombination rate. Since the TBP molecule adsorb only on a small fraction of the TiO_2 surfaces, it is likely that these sites are responsible for an increased recombina-

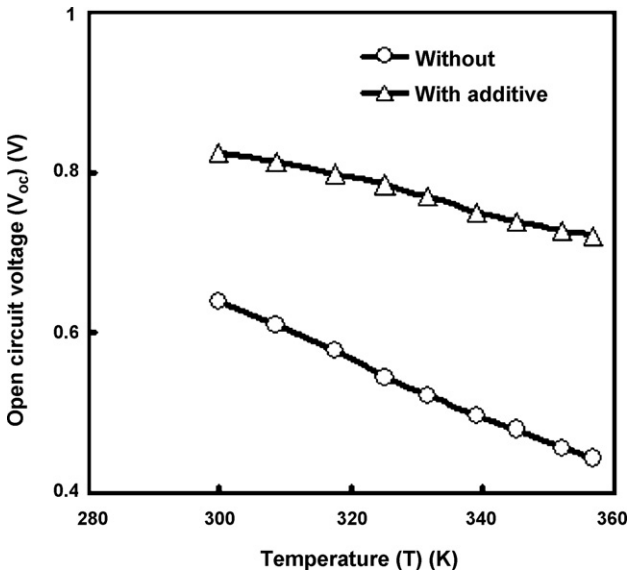

Fig. 16. Open circuit voltage as a function of temperature for DSSC with and without TBP additive in electrolyte.

tion rate in case they are not reacted by adsorbents such as TBP. This adsorption is sufficient to quench electronic states effectively in the band gap of the TiO_2. These electronic states are therefore attributed to minority sites on the TiO_2 surface, which both exhibit a higher binding energy for TBP adsorption as well as intra-band gap states that are responsible for the effective charge recombination of conduction band electrons with redox couple in electrolyte. The adsorption of TBP at those sites, the electronic states is then quenched and as a result, V_{oc} is increased by the suppression of charge carrier recombination. Because of TBP adsorption, the TiO_2 band edges shifts towards more negative side. A change in Fermi level pining before and after quenching the minority site induced intra-gap states is most likely for this change of the band edge positions.

4. Conclusions

In this article, dye sensitized solar cells (DSSCs) with different modified PEDOT:PSS as counter electrodes have been fabricated and characterized. The device with 0.2 wt% carbon black added DMSO treated PEDOT:PSS as counter electrode shows highest power conversion efficiency (PCE), which is attributed to low charge transfer resistance and improved catalytic activity. The effect of sintering temperature of TiO_2 layer on the PCE shows that the DSSC fabricated with TiO_2 sintered at 450 °C showed highest photovoltaic performances. This attributes to the high adsorption of dye and low interface resistance between TiO_2 and FTO glass and TiO_2 and redox electrolyte. The photovoltaic performance of the DSSC was studied as a function of TiO_2 film thickness, sensitization time of electrode in the dye, addition of TBP additives in the electrolyte and temperature of the device. The over all PCE of the device increases as the thickness of TiO_2 layer increases up to a certain thickness, after that it slightly decreases. This is attributed to the more dye adsorption, which leads to more photon absorption resulting higher photocurrent. The effect of TBP addition in the electrolyte is that it increases open circuit voltage without affecting much short circuit photocurrent. Results from the Mott–Schottky analysis demonstrates that the increase in photovoltage is generated from the negative shift in the conduction band edge of TiO_2 nano-crystalline, as well as the increase of back electron transfer from the conduction band of TiO_2 to tri-iodide in electrolyte. Further improvement of power conversion efficiency of dye sensitized solar cell can be achieved, with further optimization of solar cell parameters including the choice of dye sensitizers with better match with solar spectrum, dispersion of nano-particles, structures of the film, composition of electrolyte and selection of counter electrode. We have achieved the over all power conversion efficiency 5.24%, which is quite high. On the basis of the above results, we suggest that pyronine dye can be used as photosensitizer instead of ruthenium based dyes, since this dye has band gap close to that for ruthenium base dye. This will lower the cost of fabrication of DSSCs.

Acknowledgement

We are grateful to Council for Scientific and Industrial Research (CSIR), New Delhi for the financial assistance through project.

References

[1] M. Gratzel, Dye sensitized solar cells, J. Photochem. Photobiol. C 4 (2003) 145–153.
[2] K. Tennakone, G.R.R.R.A. Kumara, A.R. Kumarasinghe, P.M. Sitimanne, K.G.U. Wijayanthe, Efficient photosensitization of nanocrystalline TiO_2 films by tannins and related phenolic substances, J. Photochem. Photobiol. A 94 (1994) 217–220.
[3] B. O' Regan, M. Gratzel, A low cost, high efficiency solar cell based on dye sensitized colloidal TiO_2 films, Nature 353 (1991) 737–740.
[4] A. Hagfedt, M. Gratzel, Light-induced redox reactions in nanocrystalline systems, Chem. Rev. 95 (1995) 49–68.
[5] T. Yahannes, O. Inganas, Photoelectrochemical studies of the junction between poly[3-(4-octylphenyl) thiophene] and a redox polymer electrolyte, Sol. Energy. Mater. Sol. Cells 51 (1998) 193–202.
[6] L. Bay, L. West, B.W. Jensen, T. Jacobsen, Electrochemical reaction rates in a dye-sensitized solar cell—the iodide/tri-iodide redox system, Sol. Energy Mater. Sol. Cells 90 (2006) 341–351.
[7] G. Heywang, F. Jonas, Poly(alkylenedioxythiophene)s—new, very stable conducting polymers, Adv. Mater. 4 (1992) 116–118.
[8] J.Y. Kim, J.H. Jung, D.E. Lee, J. Joo, Enhancement of electrical conductivity of poly(3,4-ethylenedioxythiophene)/poly(4-styrenesulfonate) by a change of solvents, Synth. Met. 126 (2002) 311–316.
[9] J. Ouyang, Q. Xu, C.W. Chu, Y. Yang, G. Li, J. Shinar, On the mechanism of conductivity enhancement in poly(3,4-ethylenedioxythiophene):poly(styrene sulfonate) film through solvent treatment, Polymer 45 (2004) 8443–8450.
[10] Y. Satio, W. Kubo, T. Kitamura, Y. Wada, S. Yanagida, I^-/I_3^- redox reaction behavior on poly(3,4-ethylenedioxythiophene) counter electrode in dye-sensitized solar cells, J. Photochem. Photobiol. A 164 (2004) 153–157.
[11] D.M. de Leeuw, P.A. Kraakman, P.F.G. Bongaerts, C.M.J. Mutsaers, D.B.M. Klaassen, Electroplating of conductive polymers for the metallization of insulators, Synth. Met. 66 (1994) 263–273.
[12] S. Hao, J. Wu, Y. Huang, J. Lin, Natural dyes as photosensitizers for dye-sensitized solar cell, Sol. Energy 80 (2006) 209–215.
[13] Y. Amao, T. Komori, Bio-photovoltaic conversion device using chlorine derived from chlorophyll from Spirulina adsorbed on a nano-crystalline TiO_2 film electrode, Biosens. Bioelectron. 19 (2004) 843–847.
[14] A.S. Polo, N.Y.M. Iha, Blue sensitizers for solar cells: natural dyes from Calafate and Jaboticaba, Sol. Energy Mater. Sol. Cells 90 (2006) 1936–1944.
[15] N.J. Cherepy, G.P. Smestad, M. Gratzel, J.Z. Zhang, Ultrafast electron injection: implications for a photoelectrochemical cell utilizing an anthocyanin dye-sensitized TiO_2 nanocrystalline electrode, J. Phys. Chem. B 101 (1997) 9342–9351.
[16] C. Zafer, M. Kus, G. Turkmen, H. Dincalp, S. Demic, B. Kuban, Y. Teoman, S. Icli, New perylene derivatives dye for dye sensitized solar cells, Sol. Energy Mater. Sol. Cells 91 (2007) 427–431.
[17] N.G. Park, K. Kim, Transparent solar cells based on dye sensitized nano-crystalline semiconductors, Phys. Stat. Sol. (a) (2008) 1–10, 10.1022.pssa.200778938.
[18] T. Horiuchi, H. Miura, K. Sumioka, S. Uchida, High efficiency dye sensitized solar cells based on metal free indoline dyes, J. Am. Chem. Soc. 126 (2004) 12218–12219.
[19] M. Wang, Q.L. Zhang, Y.X. Wang, Y. Lin, X.R. Xiao, Investigation of mechanisms of enhanced open-circuit photovoltage of dye-sensitized solar cells based the electrolyte containing 1-hexyl-3-methylimidazolium iodide, Chin. Phys. Lett. 23 (2006) 724.
[20] R. Redmond, D. Fitzmaurice, Spectroscopic determination of flat band potentials for polycrystalline titania electrodes in non-aqueous solvents, J. Phys. Chem. 97 (1993) 1426–1430.
[21] M. Bergine, U.P. Krasovec, M. Jankovec, M. Topic, The effect of temperature on a propyl-methyl-imidazolium iodide electrolyte, Sol. Energy Mater. Sol. Cells 91 (2007) 821–828.
[22] J.G. Chen, H.Y. Wei, K.C. Ho, Using modified poly (3,4-ethylene dioxythiophenes):poly(styrene sulfonate) film as a counter electrode in dye sensitized solar cells, Sol. Energy Mater. Sol, Cells, doi:10.1016/solmat.2007.03.024.

[23] W.D. Callister Jr., Fundamentals of Materials Science and Engineering: An Integrated Approach, Wiley, Hoboken, 2005.
[24] N.C. Greenham, X. Peng, A.P. Alivisatos, Charge separation and transport in conjugated-polymer/semiconductor-nanocrystal composites studied by photoluminescence quenching and photoconductivity, Phys. Rev. B. 54 (1996) 17628–17637.
[25] T.W.F. Chang, S. Musikhin, L. Bakueva, L. Levina, M.A. Hines, P.W. Cyr, E.H. Sargent, Efficient excitation transfer from polymer to nanocrystals, Appl. Phys. Lett. 84 (2004) 4295.
[26] M. Pientka, V. Dyakonov, D. Meissner, A. Rogach, D. Talapin, H. Weller, L. Lusten, D. Vanderzande, Photoinduced charge transfer in composites of conjugated polymers and semiconductor nanocrystals, Nanotechnology 15 (2004) 163–170.
[27] Y. Li, Y. Cao, J. Goa, D. Wang, G. Yu, A.J. Heeger, Electrochemical properties of luminescent polymers and polymer light-emitting electrochemical cells, Synth. Met. 99 (1999) 243–248.
[28] M.K. Nazeeruddin, A. Kay, I. Podicio, R. Humphry-Baker, E. Muller, P. Liska, N. Vlacchopoulous, M. Gratzel, Conversion of light to electricity by cis-X^2bis(2,2′-bipyridyl-4,4′-dicarboxylate)ruthenium(II) charge-transfer sensitizers (X = Cl–, Br–, I–, CN–, and SCN–) on nanocrystalline titanium dioxide electrodes, J. Am. Chem. Soc. 115 (1993) 6382–6390.
[29] X.H. Zhang, C. Li, W.B. Wang, X.X. Cheng, X.S. Wang, B.W. Zhang, Photo-physical electro-chemical and photo-electrochemical properties of new azulene based dye molecules, J. Mater. Chem. 17 (2007) 642.
[30] L. Peter, Transport, trapping and interfacial transfer of electrons in dye-sensitized nanocrystalline solar cells, J. Electro-anal. Chem. 599 (2007) 233–240.
[31] M. Zukalova, A. Zukal, L. Kavan, M.K. Nazeerudin, P. Liska, M. Gratzel, Organized mesoporous TiO_2 films exhibiting greatly enhanced performance in dye-sensitized solar cells, Nano Lett. 5 (2005) 1789.
[32] J. Jiu, S. Isoda, M. Adachi, F. Wang, Preparation of TiO_2 nanocrystalline with 3–5 nm and application for dye-sensitized solar cell, J. Photochem. Photobiol. A 189 (2007) 314–321.
[33] R. Gomez, P. Salvador, Photovoltage dependence on film thickness and type of illumination in nanoporous thin film electrodes according to a simple diffusion model, Sol. Energy Mater. Sol. Cells 88 (2005) 377–388.
[34] Z.S. Wang, H. Kawauchi, T. Kashima, H. Arakawa, Significant influence of TiO_2 photoelectrode morphology on the energy conversion efficiency of N719 dye-sensitized solar cell, Coord. Chem. Rev. 248 (2004) 1381.
[35] S.Y. Huang, G. Schlichthorl, A.J. Nozik, M. Gratzel, A.J. Frank, Charge recombination in dye-sensitized nano-crystalline TiO_2 solar cells, J. Phys. Chem. B 101 (1997) 2576–2582.
[36] E.A. Schiff, Low-mobility solar cells: a device physics primer with application to amorphous silicon, Sol. Energy Mater. Sol. Cells 78 (2003) 567–595.
[37] G. Schlichthorl, S.Y. Huang, J. Sprague, A.J. Frank, Band edge movement and recombination kinetics in dye-sensitized nanocrystalline TiO_2 solar cells: a study by intensity modulated photovoltage spectroscopy, J. Phys. Chem. B. 101 (1997) 8141–8155.
[38] X. Yin, H. Zhao, L. Chen, W. Tan, J. Zhang, Y. Weng, Z. Shuai, X. Xiao, X. Zhou, X. Li, Y. Lin, The effects of pyridine derivatives additives on the interface processes at nano-crystalline TiO_2 thin film in dye sensitized solar cells, Surf. Interface Anal. 39 (2007) 809–816.
[39] R.A. Marcus, On the theory of oxidation–reduction reactions involving electron transfer. I, J. Chem. Phys. 24 (1956) 966.
[40] N. Kopidakis, N.R. Neale, A.J. Frank, Effect of an adsorbent on recombination and band-edge movement in dye-sensitized TiO_2 solar cells: evidence for surface passivation, J. Phys. Chem. B 110 (2006) 12485–12489.
[41] A. Fukul, R. Komiya, R. Yamanaka, A. Islam, L.Y. Han, Effect of a redox electrolyte in mixed solvents on the photovoltaic performance of a dye-sensitized solar cell, Sol. Energy Mater. Sol. Cells 90 (2006) 649–658.
[42] M. Gratzel, Photo-electrochemical cells, Nature 414 (2001) 338–344.
[43] K. Hara, Y. Dan-oh, C. Kasada, Y. Ohga, A. Shinpo, S. Suga, K. Sayama, H. Arakawa, Effect of additives on the photovoltaic performance of coumarin-dye-sensitized nanocrystalline TiO_2 solar cells, Langmuir 20 (2004) 4205–4210.
[44] S. Nakade, T. Kanzaki, W. Kubo, T. Kitamura, Y. Wada, S. Yanagida, Role of electrolytes on charge recombination in dye-sensitized TiO_2 solar cell. 1. The case of solar cells using the I^-/I_3^- redox couple, J. Phys. Chem. B 109 (2005) 3480–3487.
[45] M. Durr, A. Yasuda, G. Nelles, On the origin of increased open circuit voltage of dye sensitized solar cells using 4-tert-butyl pyridine as additive to electrolyte, Appl. Phys. Lett. 89 (2006) 061110.